The Effect of Geometry on the Efficiency and Hemolysis of Centrifugal Implantable Blood Pumps

Sahand Mozafari,* Mohammad A. Rezaienia,* Gordon M. Paul,* Martin T. Rothman,† Pihua Wen,* and Theodosios Korakianitis‡

The application of centrifugal pumps as heart assist devices imposes design limitations on the impeller geometry. Geometry and operating parameters will affect the performance and the hemocompatibility of the device. Among all the parameters affecting the hemocompatibility, pressure, rotational speed, blade numbers, angle, and width have significant impact on the blood trauma. These parameters directly (pressure, speed) and indirectly (geometry) affect the efficiency of the pump as well. This study describes the experimental investigation on geometric parameters and their effect on the performance of small centrifugal pumps suitable for Mechanical Circulatory Support (MCS) devices. Experimental and numerical techniques were implemented to analyze the performance of 15 centrifugal impellers with different characteristics. The effect of each parameter on the pump performance and hemolysis was studied by calculating the normalized index of hemolysis (NIH) and the shear stress induced in each pump. The results show five and six blades, 15–35° outlet angle, and the lowest outlet width that meets the required pressure rise are optimum values for an efficient hemocompatible pump. *ASAIO Journal* 2017; 63:53–59.

Key Words: pump efficiency, blood pump, congestive heart failure, hemocompatibility, hemolysis

The geometry of the impeller in a blood pump impacts the performance and hemocompatibility of the device. The typical approach to experimental evaluation of centrifugal pumps for Mechanical Circulatory Support (MCS) devices has been to consider the performance of each device in its entirety and compare it to other devices and designs. Such approach fails to differentiate between the impacts of individual parameters, which are of crucial importance to the designers. In this study, we propose a modular approach to the evaluation of geometric parameters of centrifugal pumps suitable for MCS devices.

The common technique to design a centrifugal pump is to model the pump based on previous designs using the concept of fluid dynamic similarity, also called similitude or similarity law using the $n_s - d_s$ graph. The graph shows isoefficiency lines in a log–log Cordier[1] diagram with specific speed (n_s) and specific diameter (d_s) as coordinates. The parameters n_s and d_s are characteristic dimensionless numbers indicative of the rotational speed and rotor diameter respectively.

The specific speed is given by

$$n_s = \frac{N_s \cdot \sqrt{Q}}{\left(\frac{\Delta p}{\rho}\right)^{0.75}} = \frac{\phi^{0.5}}{\psi^{0.75}} \tag{1}$$

and the specific diameter is given by

$$d_s = \frac{D \cdot \left(\frac{\Delta p}{\rho}\right)^{0.25}}{\sqrt{Q}} = \frac{\psi^{0.25}}{\phi^{0.5}}, \tag{2}$$

where N_s is the rotor speed (rad/s), Q is the volumetric flow rate (m^3/s), D is the diameter (m), ρ is the density of the working fluid (kg/m^3), Δp is the pressure difference (N/m^2) from inlet to outlet of the pump, and ϕ and ψ are flow and pressure coefficients.

Dimensionless numerical data from 100 centrifugal pumps were collected and plotted on a Cordier diagram in a previous study.[2] The numerical results were validated by testing nine pumps in a single loop test rig in steady flow conditions. In the current study, 15 impellers with various geometric parameters are designed based on dimensionless characteristic numbers of high efficiency pumps[2] and the conventional pump design method of Stepanoff.[3] The impellers were manufactured and tested in steady conditions to evaluate the effect of each geometric parameter on the pump performance and hemocompatibility. The hemocompatibility of the pumps was analyzed numerically by modeling the induced hemolysis.

There are two major models for hemolysis: strain-based and power-law model. The most common method is to relate hemolysis to the shear rate and exposure time through a power-law form. The general form of this equation is defined by

$$\mathrm{HI}(\%) = \frac{\Delta \mathrm{free\,Hb}}{\mathrm{Hb}} \times 100 = \mathrm{Ct_{exp}}^{\alpha} \sigma^{\beta}, \tag{3}$$

where HI is the hemolysis index, Hb is the total hemoglobin concentration, ΔfreeHb is the increase in plasma-free hemoglobin, σ is the shear stress, and t_{exp} is the exposure time.

From the *School of Engineering and Materials Science, Queen Mary University of London, London, United Kingdom; †Department of Cardiology. Barts and the London NHS Trust, London Chest Hospital, London, United Kingdom; and ‡Parks College of Engineering, Aviation and Technology, Saint Louis University, St. Louis, Missouri.

Submitted for consideration June 2016; accepted for publication in revised form September 2016.

Disclosures: The authors have no conflicts of interest to report.

This report is an independent research funded by the National Institute for Health Research [i4i, Turbocardia, II-LB-1111–20007]. Principal Investigator for the grant is Prof. T. Korakianitis. The views expressed in this publication are those of the authors and not necessarily those of the NHS, the National Institute for Health Research or the Department of Health. The PhD study of S. Mozafari is funded by a QMUL studentship.

Correspondence: Theodosios Korakianitis, Parks College of Engineering, Aviation and Technology, Saint Louis University, St. Louis, MO 63103. Email: korakianitis@alum.mit.edu.

DOI: 10.1097/MAT.0000000000000457

The constants α, β, and C are based on experimental data. Several research groups[4–6] have conducted experiments using the power-law equation and found the constants based on their results. Most of the published studies related to numerical estimation of hemolysis are based on the power-law model and the constants proposed by Giersiepen *et al*.[4]

There are two approaches to computational models for estimation of hemolysis: Eulerian and Lagrangian. In the Eulerian approach, the damage index is integrated over the entire computational flow domain, so the high hemolysis locations could be discerned inside the domain whereas in the Lagrangian formulation the integration is along the flow path lines.

In a previous study,[7] the two methods are compared and evaluated by experimental data in a shearing device and a clinical VAD. The study showed that both methods have high percentage errors, meaning they could not accurately predict the magnitude of the hemolysis. However the Eulerian approach had large correlation coefficients showing that it could be used to compare different devices and pump designs to each other by predicting relative hemolysis.

This study applied the developed and evaluated Eulerian scalar transport approach[4,7,8] to model the blood damage potential based on the power-law equation for 15 centrifugal pumps. The normalized index of hemolysis (NIH) was defined to express the degree of hemolysis for different design parameters in a comparative way to study the effect of each geometric parameter on the efficiency and hemolysis of small centrifugal pumps. By selecting the optimum value for each geometric parameter, a pump designer can achieve the highest possible efficiency while keeping the probability of blood complications at the minimum level.

Materials and Methods

Impeller and Volute design

The first performance estimation was made by specifying the duty frame. The flow rate and pressure rise were defined in the region of human cardiovascular system parameters corresponding to 3–7 L/min and 50–150 mm Hg, respectively. A combination of characteristics including the rotational speed, diameter, inlet flow angle, and meridional velocity ratio were determined using $n_s - d_s$ of the existing efficient pumps[2] (**Figure 1**).

The range of leading edge angle for hub and meanline were calculated relative to the leading edge blade angle. The rotational speed and the velocity triangles were then used to select the appropriate stability factor and head coefficient.[9] The trailing edge blade angle (outlet angle) varied for different models between 15° and 45° and the number of blades was selected between three and nine.

To find the optimum curvature, the meridional coordinate system was used as it is the most convenient system for axisymmetric flow and is useful for viewing the flow path. The meridional profile was divided into several streamlines and the data points of each one were achieved by using a cubic Bezier curve. The general expression of this curve is

$$B(t) = (1-t)^3 P_0 + 3(1-t)^2 t P_1 + 3(1-t) t^2 P_2 + t^3 P_3, \quad 0 \le t \le 1, \quad (4)$$

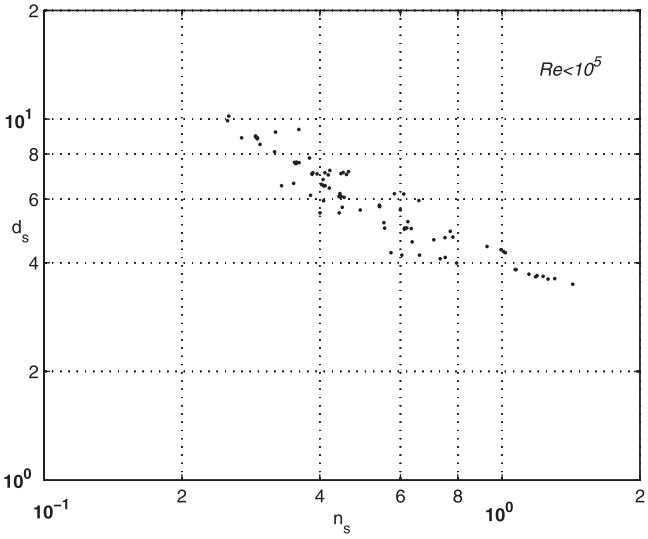

Figure 1. Highest efficiency points on n_S - d_S Cordier diagram for small centrifugal impellers.

where P and t represent a control point and the parameter value, respectively.

The leading edge and trailing edge were defined by the inlet and outlet angles and the curvature data points were modified to achieve the largest possible radius at the bend to avoid flow separation.[10–16] A small radius in meridional profile results in high velocity and flow separation and therefore reduces the efficiency.

The design parameters were optimized by creating a response surface based on the Design of Experiments (DOEs) in ANSYS Design Xplorer. The DOE was defined by determining the number of input and output values and their ranges. The aim is to get as good response surface as possible with minimum input combinations. Each combination was solved by ANSYS and based on the results, a response surface was created for each output parameter by fitting a curve through the design points. From this curve fit, the output results were investigated for input variable combinations that have not been solved for.

The results are then sorted based on the efficiency, and the most efficient pumps that also meet the pressure rise requirements are selected to be manufactured.

From the tongue (smallest radius) to the throat (largest radius) of a single volute, the circumference was divided into eight equally spaced sections and then lofted into a snail-shaped diffuser due to the difference in radii.[17]

The design procedure was then developed as a MATLAB code that generates 3D coordinates for the blade and the volute.

Computational Model

The coordinates were imported to ANSYS CFX and the incompressible Navier–Stokes equations were used to predict and calculate the flow fields in the pumps.

The model includes two domains: rotating (impeller fluid zone) and stationary (volute fluid zone). The domains are defined by creating the fluid volume around the rotor surface and inside the volute section, respectively. The rotational motion of the impeller is calculated using multiple reference frame (MRF). In this approach, the flow is assumed steady state,

the grid remains fixed and the relative velocity is calculated throughout the domain.

Boundary conditions were specified to define the rotational speed, inlet pressure, and outlet flow rate.[18] At the inlet, a relative pressure of 0 Pa was defined. It should be noted that this pressure is "relative" and not the aortic pressure (it is not physically realistic). By setting this value to 0, the resulted outlet pressure will be the pressure difference (rise) between inlet and outlet of the pump. At the outlet, a healthy human body blood flow rate (5 L/min) was imposed. In the numerical solution, a physical time step of 0.003 s is used. The solution was considered converged when the residual fell below 10^{-4}.

Three different mesh qualities were generated in a similar fashion to a study conducted by Fraser *et al*.[8] The pressure rise was taken as the output reference value and the small percentage error between the original (medium) and the fine mesh results validated the use of original mesh for all models and affirmed the mesh independence study. The k-epsilon turbulence model has been utilized. The model uses the scalable wall function to improve robustness and accuracy when the near wall mesh is fine.

Although blood is a non Newtonian fluid, for this part of the study, blood was considered as an incompressible Newtonian fluid due to shear rates higher than 100/s in centrifugal blood pumps. In this case, the non Newtonian properties of blood such as shear thinning and viscoelasticity are negligible. A density of 1050 kg/m^3 and viscosity of 0.0036 $Pa \cdot s$ were defined for the working fluid.[8]

Smaller clearance between the impeller and housing results in higher efficiency but also higher shear stress. A suitable value for this gap needs to be selected to maximize the efficiency while keeping the shear stress under the critical value. This value was selected to be 25 μm for this study.

Shear Stress and Hemolysis Model

By assuming blood as a Newtonian fluid, the scalar shear stress induced on the fluid on each boundary is defined by

$$\sigma = \left[\frac{1}{6}\sum\left(\sigma_{ii}-\sigma_{jj}\right)\left(\sigma_{ii}-\sigma_{jj}\right)+\sum\left(\sigma_{ij}\sigma_{ij}\right)\right]^{1/2} \quad (5)$$

Hemolysis is defined as the release of hemoglobin due to mechanical damage to red blood cells (RBCs) in VADs and MCS devices. The hemolysis index is a dimensionless parameter used to quantify this concept. The most common method to model the hemolysis is based on a general form of the power-law equation. The reason is the functional relationship between the two quantities, where a relative change in one results in a proportional relative change in the other one, independent of the initial size of the quantities.

The first power-law equation was used for a Couette shearing device (shear stress <255 Pa, exposure time <700 msec) and the constants α, β, and C were found to be 0.785, 2.416, and 3.62×10^{-5}, respectively.[4]

In the Eulerian scalar transport approach, $\Delta\text{free Hb}'$ was defined as a scalar and equal to $\Delta\text{free Hb}^{1/\alpha}$[7,8] and the transport equation was then proposed as

$$\frac{d(\Delta\text{free Hb}')}{dt}+v\rho\cdot\nabla(\Delta\text{free Hb}')=S, \quad (6)$$

where v is the mean inlet velocity (m/s) and S is the source term and defined as

$$S=\rho(\text{Hb}\cdot C\cdot\sigma^{\beta})^{1/\alpha} \quad (7)$$

To express the degree of hemolysis, NIH was proposed to account for the plasma volume based on the hematocrit and it is given by

$$\text{NIH}(g/100\,\text{L})=100\times\frac{\Delta\text{free Hb}}{\text{Hb}}\times(1-\text{Hct})\times k, \quad (8)$$

where Hct is the hematocrit and k is the hemoglobin content of blood and these quantities are 45% and ≈150 g/L, respectively, for a healthy person.[19]

Experimental Setup

A single loop test rig, which will be denoted as O loop hereafter, was developed in a previous study[2] for testing the manufactured models. The system consisted of the impeller housing, a clip valve to control the resistance, an electromagnetic flowmeter to measure the flow rate, pressure transducers to measure the pressure before and after the impeller, a high-speed brushless DC motor, and a controller to change the motor speed from a low value to a nominal maximum speed. The pressure difference *versus* flow rate characteristics of the pumps were recorded under a steady flow condition with a 1 kHz sampling rate.

A blood analog solution (65% water, 35% glycerol, by volume) was used as the working fluid in the O loop to obtain values of density and viscosity of working fluid representative of those of human blood at 37°C.

All the measurement process was repeated for a wide range of resistances from low (wide open, full flow) to high (closed tube, no flow).

Results

Fifteen optimized centrifugal impellers were tested and the performance characteristics were measured or calculated at different operating conditions. The highest achieved efficiency of each pump was selected for the presentation.

The nondimensional approach of the study makes the results applicable to different performance characteristics and not just specific values. Q/Q_{des} and H/H_{des} show the ratio of volumetric flow rate and pressure rise to their values at the design point.

The performance characteristics were plotted on the relevant diagrams based on their design parameters. In all cases, second order polynomial regression lines are fitted to the data points as they were the lowest order that provided a good fit to most of the data.

Figures 2 and 3 show the efficiency and head ratio (H/H_{des}) *versus* flow ratio (Q/Q_{des}) for different numbers of blades from

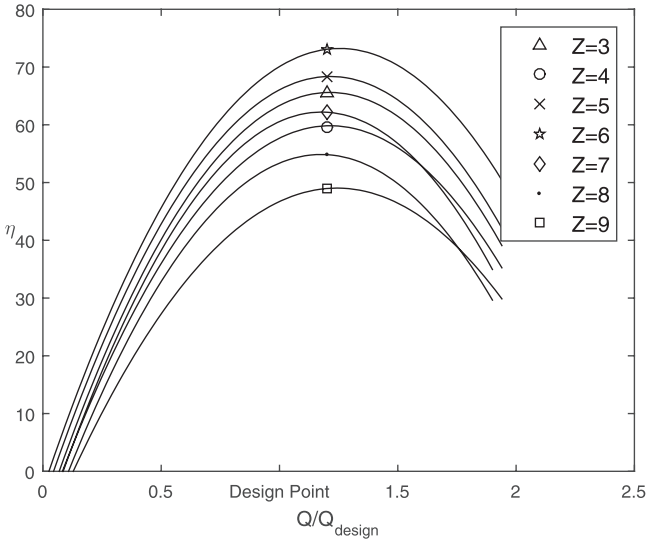

Figure 2. Experimental efficiency *vs.* Q / Q_{des} for different blade numbers.

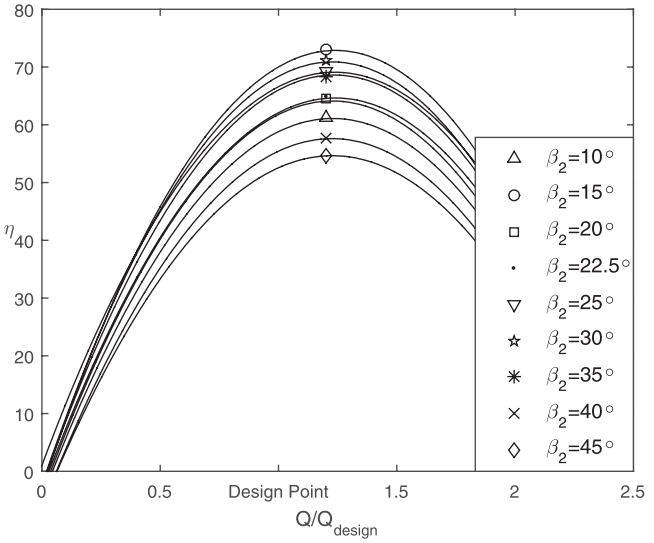

Figure 4. Experimental efficiency *vs.* Q / Q_{des} for different outlet angles.

three to nine. Six and nine blades pumps performed with the highest (>70%) and lowest efficiency (<50%), respectively. The impellers were tested in different operating conditions and the curve related to the highest efficiency for each blade number is presented in the figures.

Figures 4 and 5 show the experimental efficiency and head ratio (H / H_{des}) *versus* flow ratio (Q / Q_{des}) for different outlet angles between 15° and 45°, and **Figures 6 and 7** show the efficiency and head ratio *versus* flow ratio for outlet width between 4 and 6 mm. In summary, the efficiency for different angles has two peak points of 15° and 30° (≈70%) and the efficiency decreases as one moves away from these peak points. The trend for the outlet widths is less complex. Efficiency decreases and pressure head increases by increasing the outlet width.

The shear stress and index of hemolysis were defined and calculated numerically in ANSYS CFX based on the equations presented earlier. **Tables 1–3** show and compare the values of efficiency, pressure rise, and NIH for different pumps with different geometric parameters.

Discussion

Head ratio, flow ratio, and efficiency were measured and calculated under steady conditions to obtain the performance characteristics of the models. One of the pumps was also tested in the cardiovascular flow emulator rig presented in references 2, 20–22 to compare the steady and transient flow conditions. The steady flow showed a pressure rise of 90.84 mm Hg at 5 L/min. The same pump operated in transient flow and resulted in a maximum and minimum pressure rise of 115 and 78 mm Hg, respectively, and an average pressure rise of 90.72 mm Hg.

Number of Blades

Figure 2 shows the effect of blade number on the pump efficiency. The effect of blade number on the performance depends on the viscosity of the working fluid. For lower viscosities, the number of blades has a larger impact on the performance than that of higher viscosity fluids. The kinematic

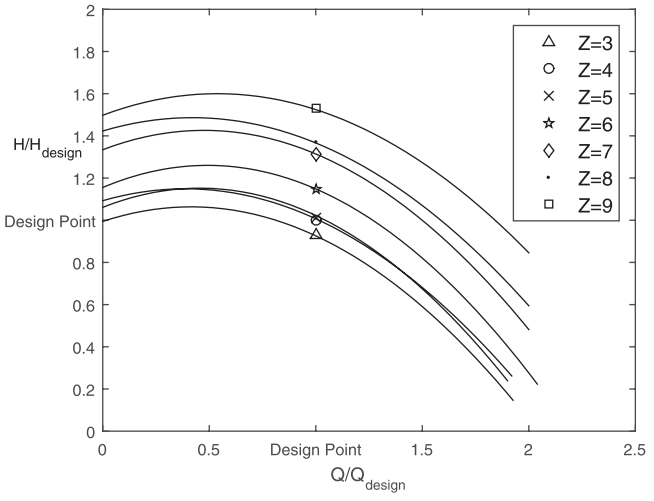

Figure 3. H / H_{des} *vs.* Q / Q_{des} for different blade numbers.

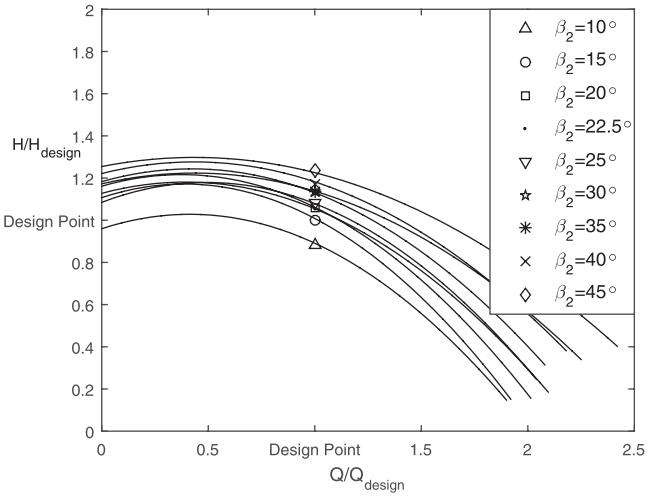

Figure 5. H / H_{des} *vs.* Q / Q_{des} for different outlet angles.

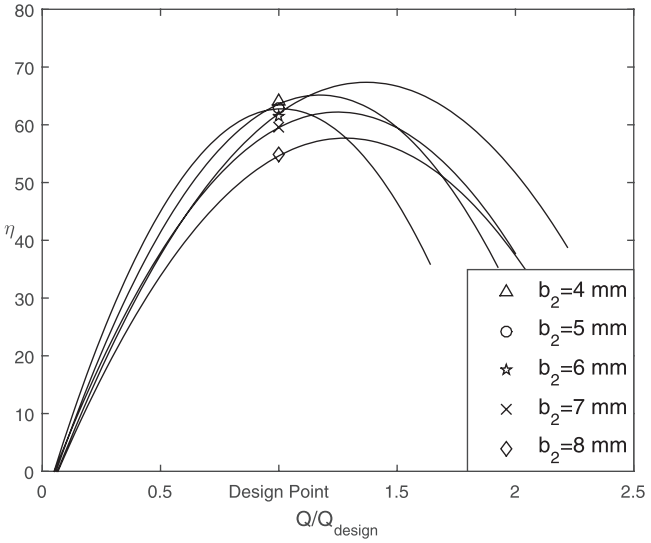

Figure 6. Experimental efficiency *vs.* Q / Q_{des} for different outlet widths.

viscosity of blood at normal body temperature (37°C) is 2.65 mm^2/s which is low compared with other fluids being pumped by centrifugal pumps. Based on **Figure 2**, six, five, and three blades were the most efficient pumps, whereas nine and eight blades performed with the lowest efficiencies. The maximum difference is between the highest (six blades) and lowest (nine blades) efficiencies and is ≈24%. The reason is the slip factor that generally increases by increasing the number of blades, therefore accounts for one of the most important parameters for losses. Based on the theoretical and experimental equations for slip factor, the ideal flow guidance could be achieved by increasing the number of blades, so the flow leaves the impeller outlet at the exact blade angle. However, beyond a particular value, the slip factor decreases due to increased blockage area. According to the results, this particular optimum value is six. This value is considered a balance between the excessively high surface friction in pumps with too many blades and unguided diffusion in pumps with too few blades.

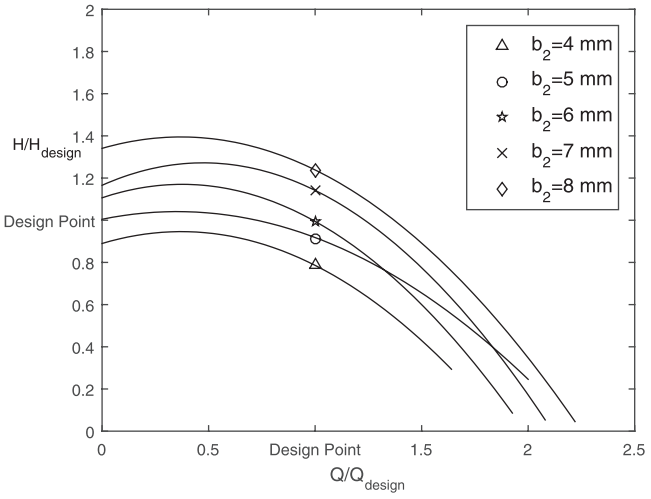

Figure 7. H / H_{des} *vs.* Q / Q_{des} for different outlet widths.

Table 1. NIH for Different Number of Blades at the Operating Condition

Number of Blades	Pressure (mm Hg)	Efficiency (%)	NIH (g/100 L)
3	65.1	63.38	0.006578
4	70.3	56.47	0.007205
5	71.4	65.17	0.007964
6	80.5	70.87	0.008422
7	92.0	61.89	0.009897
8	96.7	54.66	0.010117
9	107.2	45.23	0.017881

NIH, normalized index of hemolysis.

Figure 3 shows the effect of blade number on head ratio. As expected, a higher number of blades results in higher head ratio. Experiments show that impellers with five and six blades could meet the design point pressure rise at the flow rate of 5 L/min.

Outlet Angle

Figure 5 shows the effect of blade outlet angle on the head ratio. Higher outlet angle results in higher pressure ratio at the same rotational speed. The reason is the relationship between the total head and the peripheral velocity at the tip of the blade. The total head at any radius, which is equally divided between static and kinetic heads, is proportional to the square of peripheral velocity. By increasing the outlet angle, the fluid leaves the impeller at a higher inclination and therefore at a higher velocity. This higher velocity results in higher pressure rise at the outlet. According to the test results, the difference is ≈25 mm Hg between the minimum and maximum values which are obtained for 10° and 45° pumps, respectively. This effect is relatively smaller than that of change in number of blades.

Based on **Figures 4 and 5**, angles 15° and 30° have the highest efficiencies but will result in different values of pressure rise. A 15° outlet angle results in the desired pressure rise at the design point. Based on the application and installation type of VADs and the favorable pressure rise in the system, the relevant outlet angle could be selected by the designer.

Outlet Width

Figures 6 and 7 show the effect of outlet width on the pump performance. An increase in outlet width will result in a larger outlet area and therefore higher flow rate. To keep this flow rate for comparison, there is need for higher resistance in the

Table 2. NIH for Different Outlet Angles at the Operating Condition

Outlet Angle (°)	Pressure (mm Hg)	Efficiency (%)	NIH (g/100 L)
10	61.7	59.13	0.005115
15	70.0	70.87	0.006647
20	73.8	62.62	0.006661
22.5	74.0	63.63	0.006930
25	75.6	66.37	0.007009
30	79.0	68.17	0.007401
35	79.5	64.88	0.007801
40	82.0	55.12	0.009563
45	86.4	51.10	0.011230

NIH, normalized index of hemolysis.

Table 3. NIH for Different Outlet Widths at the Operating Condition

Outlet Width (mm)	Pressure (mm Hg)	Efficiency (%)	NIH (g/100 L)
4.0	55.0	64.09	0.003122
5.0	63.8	62.83	0.003943
6.0	69.6	61.57	0.006118
7.0	80.1	59.67	0.006284
8.0	86.7	54.77	0.008951

NIH, normalized index of hemolysis.

system. This higher resistance results in higher pressure rise. Therefore by increasing the outlet width and keeping the flow rate constant at the design point, the pressure increases and the efficiency decreases. This pattern is consistent for all impellers with no exceptions. The optimum value for the outlet width is the smallest value that meets the required pressure.

Hemolysis

Based on the values of linear velocity on the surface of the impeller (4–8 m/s) and inside the pipes (0.2 m/s), the shear stress in the pipe is negligible compared with that on the gap between the impeller and housing and on the impeller surface (20 to 40 times larger on the impeller).

Based on the values from **Table 1**, by increasing the number of blades at a constant rotational speed, the pressure increases and results in higher shear stress and NIH. To compare the impellers at the same pressure rise, a lower rotational speed is needed for higher number of blades and it leads to a lower shear stress and NIH. Therefore higher number of blades at low rotational speeds and lower number of blades at high rotational speeds will have more or less the same effect on hemolysis and shear stress. The priority is lower number of blades at a higher rotational speed to keep the surface area minimum and lower the probability of hemolysis.

Table 2 shows the same quantities for different outlet angles. Based on the results, the effect of change in outlet angle on hemolysis is much smaller than that of number of blades. Higher outlet angle at the same rotational speed will result in a slight increase in pressure rise and therefore shear stress and NIH. One way to find the most hemocompatible angle is to lower the needed rotational speed by increasing the angle to an optimum value. This value is an angle that leads to a pressure rise close to design point and NIH lower than 0.01 g/100 L.[23] Based on the values on **Table 2**, an outlet angle of 30° will perform with high efficiency, demanded pressure rise, and a safe zone for hemolysis.

The results from last table show a higher probability of hemolysis by increasing the outlet width. The reason is the higher pressure rise and therefore higher shear stress and NIH. **Table 3** indicates that all values of outlet widths are suitable and have NIH lower than the critical value.

Conclusion

It is recommended to pick the lower number of blades and increase the rotational speed until the desired pressure rise is achieved. Based on the results, five blades is a suitable choice for this application. Outlet angles 15° and 30° performed with highest efficiencies and 30° impeller was found to be more hemocompatible. All outlet widths performed under the critical value for hemolysis and based on the performance curves, 4 mm results in highest efficiency. So the optimum design value would be the smallest width that meets the pressure requirement.

Using these results, a pump designer can study the effects and select each geometric parameter based on their desired output.

References

1. Cordier O: Ahnlichkeitsbedingungen fur Stromungsmaschinen, In: Brennstoff-Warme-Kraft, Zeitschrift fur Energiewirtschaft und technische Uberwachung, Fachheft Stromungsmaschinen, Band 5, Heft Nr.10, Oktober 1953, Düsseldorf.
2. Korakianitis T, Rezaienia MA, Paul GM, Rahideh A, Rothman MT, Mozafari S: Optimization of centrifugal pump characteristic dimensions for mechanical circulatory support devices. *ASAIO J* 62: 545–551, 2016.
3. Stepanoff AJ: *Centrifugal and Axial Flow Pumps*. New York, NY, John Wiley & Sons, 1957.
4. Giersiepen M, Wurzinger LJ, Opitz R, Reul H: Estimation of shear stress-related blood damage in heart valve prostheses–in vitro comparison of 25 aortic valves. *Int J Artif Organs* 13: 300–306, 1990.
5. Heuser G, Opitz R: A Couette viscometer for short time shearing of blood. *Biorheology* 17: 17–24, 1980.
6. Zhang T, Taskin ME, Fang HB, *et al*: Study of flow-induced hemolysis using novel Couette-type blood-shearing devices. *Artif Organs* 35: 1180–1186, 2011.
7. Taskin ME, Fraser KH, Zhang T, Wu C, Griffith BP, Wu ZJ: Evaluation of Eulerian and Lagrangian models for hemolysis estimation. *ASAIO J* 58: 363–372, 2012.
8. Fraser KH, Zhang T, Taskin ME, Griffith BP, Wu ZJ: A quantitative comparison of mechanical blood damage parameters in rotary ventricular assist devices: shear stress, exposure time and hemolysis index. *J Biomech Eng* 134: 081002, 2012.
9. Mansour M, Chokani N, Kalfas AI, Abhari RS: Unsteady entropy measurements in a high-speed radial compressor. ASME. *J Eng Gas Turb Power* 130: 021603–021603-9, 2008.
10. Korakianitis T, Hamakhan IA, Rezaienia MA, Wheeler APS, Avital EJ, Williams JJR: Design of high efficiency turbomachinery blades for energy conversion devices with the three-dimensional prescribed surface curvature distribution blade design (CIRCLE) method. *Appl Energy* 89, 215–227, 2012.
11. Korakianitis T, Rezaienia MA, Hamakhan IA, Avital EJ, Williams JJR: Aerodynamic improvements of wind turbine airfoil geometries with the prescribed surface curvature distribution blade design (CIRCLE) method. *J Eng Gas Turb Power* 134: 082601–082601-9, 2012.
12. Pachidis V, Pilidis P, Texeira J, Templalexis I: A comparison of component zooming simulation strategies using streamline curvature. Proceedings of the Institution of Mechanical Engineers, Part G: Journal of Aerospace Engineering, 221, 1–15, 2007.
13. Massardo A, Satta A, Marini M: Axial-flow compressor design optimization. part 2. throughflow analysis. Trans ASME. *J Turbomach* 112, 405–410, 1990.
14. Korakianitis T, Rezaienia M, Hamakhan I, Wheeler A: Two- and three-dimensional prescribed surface curvature distribution blade design (CIRCLE) method for the design of high efficiency turbines, compressors, and isolated airfoils. *J Turbomach* 135: 041002–041002-11, 2013.
15. Hamakhan IA, Korakianitis T: Aerodynamic performance effects of leading edge geometry in gas turbine blades. *Appl Energy* 87, 1591–1601, 2010.
16. Zachos P, Pilidis P, Kalfas A: Analysis of turbine performance degradation effects due to geometry variations between actual components and design intent. *Aeronaut J*, 114, 569–578, 2010.
17. Boehning F, Timms DL, Amaral F, *et al*: Evaluation of hydraulic radial forces on the impeller by the volute in a centrifugal rotary blood pump. *Artif Organs* 35: 818–825, 2011.

18. Pachidis V, Pilidis P, Talhouarn F, Kalfas A, Templalexis I: A fully integrated approach to component zooming using computational fluid dynamics. *J Eng Gas Turb Power* 128, 579–584, 2006.
19. Arora D, Behr M, Pasquali M: Hemolysis estimation in a centrifugal blood pump using a tensor-based measure. *Artif Organs* 30: 539–547, 2006.
20. Shi Y, Korakianitis T: Numerical simulation of cardiovascular dynamics with left heart failure and in-series pulsatile ventricular assist device. *Artif Organs* 30: 929–948, 2006.
21. Rezaienia MA, Rahideh A, Rothman MT, Sell SA, Mitchell K, Korakianitis T: *In vitro* comparison of two different mechanical circulatory support devices installed in series and in parallel. *Artif Organs* 38: 800–809, 2014.
22. Rezaienia MA, Rahideh A, Alhosseini Hamedani B, Bosak DE, Zustiak S, Korakianitis T: Numerical and *in vitro* investigation of a novel mechanical circulatory support device installed in the descending aorta. *Artif Organs* 39: 502–513, 2015.
23. Chan CH, Pieper IL, Hambly R, *et al*: The CentriMag centrifugal blood pump as a benchmark for *in vitro* testing of hemocompatibility in implantable ventricular assist devices. *Artif Organs* 39: 93–101, 2015.